



OPEN ACCESS

EDITED BY

Salem Hannoun,
American University of Beirut, Lebanon

REVIEWED BY

Wenbo Sun,
Zhongnan Hospital, Wuhan University, China
Huajun Liang,
University of Maryland, United States

*CORRESPONDENCE

Nathan W. Churchill
✉ nchurchill.research@gmail.com

RECEIVED 14 May 2024

ACCEPTED 22 July 2024

PUBLISHED 06 August 2024

CITATION

Churchill NW, Roudaia E, Chen JJ, Sekuler A, Gao F, Masellis M, Lam B, Cheng I, Heyn C, Black SE, MacIntosh BJ, Graham SJ and Schweizer TA (2024) Effects of post-acute COVID-19 syndrome on cerebral white matter and emotional health among non-hospitalized individuals. *Front. Neurol.* 15:1432450. doi: 10.3389/fneur.2024.1432450

COPYRIGHT

© 2024 Churchill, Roudaia, Chen, Sekuler, Gao, Masellis, Lam, Cheng, Heyn, Black, MacIntosh, Graham and Schweizer. This is an open-access article distributed under the terms of the [Creative Commons Attribution License \(CC BY\)](https://creativecommons.org/licenses/by/4.0/). The use, distribution or reproduction in other forums is permitted, provided the original author(s) and the copyright owner(s) are credited and that the original publication in this journal is cited, in accordance with accepted academic practice. No use, distribution or reproduction is permitted which does not comply with these terms.

Effects of post-acute COVID-19 syndrome on cerebral white matter and emotional health among non-hospitalized individuals

Nathan W. Churchill^{1,2,3*}, Eugenie Roudaia⁴, J. Jean Chen^{4,5,6}, Allison Sekuler^{4,7,8}, Fuqiang Gao⁹, Mario Masellis^{4,9,10}, Benjamin Lam^{4,9,10}, Ivy Cheng^{11,12,13}, Chris Heyn^{9,14}, Sandra E. Black^{4,9,10}, Bradley J. MacIntosh^{5,9,15,16}, Simon J. Graham^{5,9,15} and Tom A. Schweizer^{1,2,17}

¹Brain Health and Wellness Research Program, St. Michael's Hospital, Unity Health Toronto, Toronto, ON, Canada, ²Keenan Research Centre for Biomedical Science of St. Michael's Hospital, Unity Health Toronto, Toronto, ON, Canada, ³Physics Department, Toronto Metropolitan University, Toronto, ON, Canada, ⁴Rotman Research Institute, Baycrest Academy for Research and Education, Toronto, ON, Canada, ⁵Department of Medical Biophysics, University of Toronto, Toronto, ON, Canada, ⁶Institute of Biomedical Engineering, University of Toronto, Toronto, ON, Canada, ⁷Department of Psychology, University of Toronto, Toronto, ON, Canada, ⁸Department of Psychology, Neuroscience and Behaviour, McMaster University, Hamilton, ON, Canada, ⁹Hurvitz Brain Sciences Program, Sunnybrook Research Institute, Toronto, ON, Canada, ¹⁰Division of Neurology, Department of Medicine, Sunnybrook Health Sciences Centre, University of Toronto, Toronto, ON, Canada, ¹¹Evaluative Clinical Sciences, Sunnybrook Research Institute, Toronto, ON, Canada, ¹²Integrated Community Program, Sunnybrook Research Institute, Toronto, ON, Canada, ¹³Department of Medicine, University of Toronto, Toronto, ON, Canada, ¹⁴Department of Medical Imaging, University of Toronto, Toronto, ON, Canada, ¹⁵Physical Sciences Platform, Sunnybrook Research Institute, Toronto, ON, Canada, ¹⁶Computational Radiology and Artificial Intelligence Unit, Division of Radiology and Nuclear Medicine, Oslo University Hospital, Oslo, Norway, ¹⁷Faculty of Medicine (Neurosurgery), University of Toronto, Toronto, ON, Canada

Introduction: Post-acute COVID syndrome (PACS) is a growing concern, given its impact on mental health and quality of life. However, its effects on cerebral white matter remain poorly understood, particularly in non-hospitalized cohorts. The goals of this cross-sectional, observational study were to examine (1) whether PACS was associated with distinct alterations in white matter microstructure, compared to symptom-matched non-COVID viral infection; and (2) whether microstructural alterations correlated with indices of post-COVID emotional health.

Methods: Data were collected for 54 symptomatic individuals who tested positive for COVID-19 (mean age 41 ± 12 yrs., 36 female) and 14 controls who tested negative for COVID-19 (mean age 41 ± 14 yrs., 8 female), with both groups assessed an average of 4–5 months after COVID testing. Diffusion magnetic resonance imaging data were collected, and emotional health was assessed via the NIH emotion toolbox, with summary scores indexing social satisfaction, well-being and negative affect.

Results: Despite similar symptoms, the COVID-19 group had reduced mean and axial diffusivity, along with increased mean kurtosis and neurite dispersion, in deep white matter. After adjusting for social satisfaction, higher levels of negative affect in the COVID-19 group were also correlated with increased mean kurtosis and reduced free water in white matter.

Discussion: These results provide preliminary evidence that indices of white matter microstructure distinguish PACS from symptomatic non-COVID infection. Moreover, white matter effects seen in PACS correlate with the severity of emotional sequelae, providing novel insights into this highly prevalent disorder.

KEYWORDS

white matter, COVID-19, emotions, DTI, DKI, NODDI

1 Introduction

Severe Acute Respiratory Syndrome Coronavirus-2 (SARS-CoV-2) and the associated Coronavirus Disease 2019 (COVID-19) represent an ongoing health crisis (1), with long-lasting health effects among survivors. Of growing concern is post-acute COVID syndrome (PACS), in which symptom impairments last well beyond the acute phase of infection; typical definitions involve COVID-related symptoms that persist over 12 weeks post-infection (2, 3). This condition is highly prevalent, with persistent symptoms reported in over 30% of COVID-19 survivors (4). Lasting issues related to mood and psychological distress are also common features of PACS (5), raising concerns about emotional health and long-term quality of life. The biological processes that underlie PACS are understudied, however, particularly for non-hospitalized cohorts. Evidence continues to mount that the brain is vulnerable to COVID-19 (6), but it is uncertain to what extent persistent symptoms represent injury sustained during acute infection, persistent inflammatory effects, and/or psychological sequelae.

A better understanding of PACS pathophysiology is needed to characterize this disorder. In this respect, cerebral white matter is of interest, as it is the anatomical substrate supporting inter-regional communication and it is vulnerable to diffuse disease processes. The heterogeneity and multi-domain nature of post-COVID neurological symptoms (7) further supports the presence of diffuse white matter pathophysiology as a contributing factor (8, 9). Such post-COVID changes in white matter microstructure can be measured using diffusion-weighted magnetic resonance imaging (dMRI), which obtains brain images sensitive to the local diffusion properties of water. DMRI techniques have been shown to be sensitive to a variety of disease processes (10), including inflammation, axonal degeneration, demyelination and edema.

Standard dMRI techniques such as diffusion tensor imaging (DTI) quantify water diffusion properties of fractional anisotropy (FA), reflecting the directionality of water movement, and mean diffusivity (MD), reflecting the rate of movement; the latter may be split into axial diffusivity (AD) and radial diffusivity (RD) components, reflecting movements parallel and perpendicular to the primary axis of diffusion (11). This approach models tissue water as a single compartment with anisotropic Gaussian diffusion. More advanced models are also used, in which images with different diffusion weightings are acquired. This includes diffusion kurtosis imaging (DKI) (12), which estimates mean kurtosis (MK), reflecting departure from Gaussianity. Other techniques model multiple tissue water compartments, such as neurite orientation density and dispersion imaging (NODDI) (13). This technique estimates the fractional intracellular water volume (V_{IC}) and isotropic free water volume (V_{ISO}), along with an orientation dispersion index (ODI) measuring the geometric organization of neurites. Research is increasingly

using dMRI to study COVID-19, but much remains unknown. Studies have used dMRI to assess individuals who have recovered from COVID-19 in hospitalized and non-hospitalized cohorts (14–18), along with cohorts with persistent post-COVID symptoms (19), usually compared to healthy uninfected controls. Less is known about dMRI effects among non-hospitalized PACS cohorts, and it is presently unclear to what extent such effects differ from non-COVID viral infection. This is an important issue to investigate, in order to establish neural involvement that is specific to COVID-19, as opposed to a reflection of general systemic inflammation (20, 21). Moreover, the relationship of dMRI with clinical measures of emotional health has been understudied in PACS, making it unclear to what extent white matter pathophysiology underlies these highly prevalent issues (5).

The present study investigated these knowledge gaps using dMRI data collected from self-isolating individuals who tested positive for SARS-CoV-2 and subsequently experienced persistent symptoms. They were compared to a control group that had cold or flulike symptoms and tested negative for SARS-CoV-2, with both groups imaged an average of 4–5 months after testing for COVID-19 infection. For the COVID-19 group, associations were further tested between dMRI and measures of emotional health, collected via the National Institutes of Health (NIH) Toolbox (22), a computerized platform that assesses behavioral and neurologic function. It was hypothesized that, despite both groups reporting post-infection symptoms, the COVID-19 group would show increased FA, MK and ODI, and reduced MD, AD, RD and V_{IC} , as a consequence of COVID-related neural injury (15, 16, 23), and that the effects would be greater for those in the COVID-19 group with poorer indices of emotional health.

2 Materials and methods

2.1 Study participants

Study participants were recruited through multiple sources, including the emergency department at a single Canadian hospital, physician referral and community advertisements, following the protocol outlined in (24). Candidate participants were identified via electronic records and contacted by phone or email to verify eligibility and to obtain consent to participate. They were eligible if between 20 and 75 years of age and living independently, and they had documented evidence of a positive or negative COVID-19 diagnosis, obtained via nasopharyngeal or oropharyngeal swab with real-time reverse transcription polymerase chain reaction (PCR) testing, conducted at a provincially-approved facility (25). They were excluded from the study if they previously had a diagnosis of dementia,

neurologic disorder, severe psychiatric illness, traumatic brain injury or ongoing unstable cardiovascular disease, or contraindication to MRI (e.g., claustrophobia or ferromagnetic implant). Both COVID-positive participants and COVID-negative controls were assessed a minimum of 14 days post-infection to ensure that they were non-infectious, and they were required to be symptomatic at the time of assessment (see section 2.3 below for further details of symptom assessment). The COVID-positive group was further required to have been non-hospitalized and to have self-isolated following a positive diagnosis. Recruitment and data collection were carried out in accordance with the Canadian Tri-Council Policy Statement 2 and institutional research ethics board, with participants giving free and written informed consent.

Participant recruitment and data collection was carried out between May 2020 and December 2021, which was predominantly during the initial “wild-type” infection wave (26). In addition, 62/68 participants were scanned prior to public vaccine availability in Ontario, which was initiated in April 2021 (27). Within the study cohort, 4 participants (all with COVID-19) were vaccinated prior to the study-relevant viral infection, and only 1 study participant (with COVID-19) had a previous lab-confirmed COVID-19 infection, identified 580 days prior to the study-relevant infection. Initial testing did not find these participants to be significant outliers in terms of demographics, clinical data or dMRI data, and thus were retained for further analysis.

2.2 Magnetic resonance imaging data

Participants were imaged at a single site using a 3 Tesla MRI system (Magnetom Prisma, Siemens Healthineers). Diffusion imaging involved three acquisitions of 2D echo-planar imaging data (2.5 mm isotropic voxels, obtained via 96×96 matrix with 60 oblique-axial slices, 62/4300 ms TE/TR, 30 diffusion encoding directions and 4 b0 scans, A >> P phase encoding); imaging was obtained for b -values of 700, 1,400 and 2,100 s/mm². An additional pair of unweighted b0 images with reversed phase encoding (P >> A) were also collected prior to diffusion-weighted imaging to correct for spatial distortions. The data were processed using a hybrid pipeline that included FSL (FMRIB software library),¹ DTI-TK² and in-house software (see Appendix 1 for details). DTI parameters were obtained for each participant using the FSL *dtifit* program, including fractional anisotropy (FA), mean diffusivity (MD), axial diffusivity (AD) and radial diffusivity (RD), for each of the diffusion weightings. The set of diffusion weightings was also used to calculate mean kurtosis (MK) with *dtifit* and NODDI parameters were estimated using the Matlab toolbox.³ The latter parameter set included volume fractions of intracellular neurite water (V_{IC}) and isotropic free water (V_{ISO}), along with the orientation dispersion index (ODI) assessing the spatial organization of neurites. The diffusion parameter maps were warped into Montreal Neurological Institute (MNI) standard space and resampled to 3 mm isotropic voxel resolution, using DTI-TK's tensor-based diffeomorphic alignment tools to register to the IIT Human Brain Atlas' mean tensor template (28).

Subsequent voxel-wise analyses were restricted to a mask of regions with mean FA > 0.30, consisting of probable white matter. Before analysis, the resampled parameter maps were also spatially smoothed using a 3D Gaussian kernel with 6 mm full width at half maximum (FWHM), to reduce voxel noise and make analyses robust to minor spatial variability between participants. Outlier testing found no participants with abnormal head motion or abnormal diffusion signal changes, and only one participant (COVID-19) whose MK and V_{ISO} maps had abnormal values (suggesting poor fit), which were excluded from analysis. Post-hoc testing of head motion also found no significant confounding effects for the main study analyses (see Appendix 1 for details). In subsequent analyses, for DTI parameter maps, results are presented for $b = 1,400$ s/mm² only, as minimal differences were seen in other acquisitions; whereas MK and NODDI parameter estimates were computed from all three b -value shells.

2.3 Analysis of clinical and demographic data

Participant demographics were tabulated including age, sex, years of education, days from symptom onset to imaging, and days from PCR test to imaging. Participants also completed a questionnaire evaluating symptom status for 9 items: fever, cough, sore throat, shortness of breath, fatigue, gastrointestinal issues, problems with smell/taste, headache and “other.” They reported whether each symptom (1) was absent, (2) had occurred but resolved, or (3) was currently ongoing. Symptoms were identified if onset was concurrent with, or subsequent to, the study-relevant viral infection and PCR test. Participants also completed the emotional health component of the NIH Toolbox (29). This computerized program provides a battery of questionnaires assessing emotions, attitudes and inter-personal relationships. Test scores are aggregated into domain-specific summary measures, including social satisfaction (SocSat), well-being (WelBei) and negative affect (NegAff), before conversion to demographic-adjusted normalized T-scores (mean = 50, SD = 10). NIH Toolbox data were not collected for four participants (1 control, 3 COVID-19), hence they were excluded from emotional health analyses.

After assessing the normality of demographic and clinical variables by comparing skewness and kurtosis values against a simulated null distribution (5,000 resamples), means and standard deviations were reported for measures that did not deviate from normality and medians with upper and lower quartiles were reported for those that did. For analyses of both clinical and neuroimaging data, bootstrapping was used to estimate the confidence intervals and p -values for effects of interest. This approach randomly resamples on participants with replacement (2000 iterations) and recomputes the test statistic of interest for each sample, thereby providing an empirical sampling distribution (30). This non-parametric technique provides a highly flexible approach to statistical inference, which does not depend on modeling assumptions common to many parametric models, such as the normality of residuals and homogeneity of variance; the latter is particularly important in cases of unbalanced group sizes (31). The frequency of ongoing and resolved individual symptoms was also reported, with bootstrapped 95% confidence intervals (95% CIs), along with average number of symptoms reported, for “ongoing” symptoms and for “combined” symptoms (ongoing plus resolved). A series of 2-sample bootstrap analyses (2000 iterations)

1 <https://fsl.fmrib.ox.ac.uk/fsl>

2 dti-tk.sourceforge.net

3 nitrc.org/projects/noddi_toolbox

tested for group differences in demographics (two-tailed), symptom reporting frequencies, symptom counts, and emotional summary scores. For the emotional scores, COVID-19 and control groups were further compared to the normative reference, via 1-sample bootstrap analyses of the difference from the normative mean ($T=50$). Summary statistics were reported for all analyses, including group differences, their standard errors (SEs), bootstrap ratio values (BSR; this is a z-scored statistic of effect, calculated via the ratio of bootstrap mean/SE), along with two-tailed percentile p -values. Differences of means were reported for variables that did not deviate from normality, and differences of medians were reported for those that did, with significant effects identified at $p < 0.05$, unadjusted.

2.4 Effects of COVID-19 on dMRI data

For each dMRI parameter, voxel-wise analyses were performed assessing the mean difference between COVID-19 and control groups. Group differences were estimated using a general linear model (GLM), with covariates adjusting for age and sex, as these parameters may influence dMRI values (32–34). Significant voxels were identified based on the bootstrapping of group effects (2000 iterations), adjusted for multiple comparisons: voxels were retained where the 99.5%CI did not include zero (corresponding to a threshold of $p < 0.005$, two-tailed), followed by cluster-size thresholding at $p < 0.05$ using Analysis of Functional NeuroImages (AFNI) programs *3dFWHMx* to estimate spatial smoothness and *3dClustSim* to estimate a minimum cluster-size threshold. For significant voxels, effect sizes were reported as z-scored BSR values. For dMRI parameters with significant effects, post-hoc summaries of group effects were obtained by averaging over significant voxels and refitting a GLM, with reporting of effects and bootstrapped 95%CIs.

2.5 Association of emotional health with dMRI data in COVID-19

To evaluate COVID-related associations between dMRI data and the three emotional health summary scores, a regression-weighted composite score was constructed that most strongly differentiated between COVID-19 and control groups. This approach was chosen to examine the relationship between dMRI parameters and emotional health for individuals with PACS, while avoiding excessive analysis of potentially redundant variables – analyses instead focused on the single predictor that encodes the most information about COVID-19 status. Composite scoring was achieved via linear discriminant analysis, regressing COVID-19 status (binary) onto the summary scores. All possible subsets of the three summary scores (SocSat, WelBei, NegAff) were examined as predictors of COVID-19 status, and the resulting models were compared using the Akaike information criterion with small sample correction (AICC) (35). The optimal discriminant model was identified that minimized the AICC score, and performance was measured relative to other models in terms of the difference scores (Δ AICC) and relative likelihood values (LAICC). See Appendix 2 for full model comparison details, along with the results of variable importance testing.

The set of participant scores produced by the linear discriminant model were retained as the linear composite score

that optimally discriminated between COVID-19 and control groups. Effect sizes were reported for this NIH composite score, in terms of the mean group difference, bootstrapped 95%CI, BSR and p -value. To assess the relationship between this score and post-COVID symptoms, it was correlated against individual symptoms within the COVID-19 group, for “ongoing” status only and for “combined” status (ongoing plus resolved). The composite was also correlated against total “ongoing” and “combined” symptom counts. Spearman correlation coefficients were calculated, with bootstrapped 95%CIs and p -values, and significance was assessed at a false discovery rate (FDR) threshold of 0.05, in order to control for multiple comparisons.

To assess the relationship between the emotional sequelae and post-COVID brain physiology, voxel-wise bootstrapped partial correlations were then conducted, correlating dMRI measures against the NIH composite score. This was assessed within the COVID-19 group, with covariates adjusting for age and sex. Significant voxels were identified as in the previous section, based on 99.5%CIs adjusted for multiple comparisons at $p < 0.05$ using cluster-size thresholding. For significant regions, the effect sizes were again reported using z-scored BSR values. For dMRI parameters with significant effects, post-hoc summaries of effect sizes were obtained by averaging over significant voxels and recomputing the partial correlations of dMRI values with emotional composite scores, and bootstrapped 95%CIs.

3 Results

3.1 Analysis of clinical and demographic data

A total of 54 COVID-positive participants and 14 COVID-negative controls had been recruited and scanned. Table 1 shows that the groups had similar age ranges, proportions of male/female participants and years of education. None of the study participants had medical comorbidities, and none of the participants in the COVID-19 group had severe respiratory symptoms requiring medical intervention. In terms of symptoms, both groups showed moderately high, and largely comparable, reporting rates for individual symptoms, both ongoing and resolved, along with comparable total symptom counts. The only notable group difference in Table 1 was a higher prevalence of ongoing headache symptoms in the COVID-19 group.

Examining NIH summary scores, moderately strong correlations were observed between SocSat and WelBei (mean and 95%CI: 0.52, [0.36, 0.66]), between SocSat and NegAff (−0.58, [−0.72, −0.41]), and between WelBei and NegAff (−0.75, [−0.84, −0.62]). In general, group means of the summary scores showed modest but significant differences from the normative mean ($T=50$) in SocSat, for both COVID-19 (−4.1 [−6.3, −1.6], BSR = −3.33, $p=0.006$) and controls (−8.7, [−15.5, −2.0], BSR = −2.59, $p=0.008$); in WelBei, for both COVID-19 (−5.8, [−7.6, −3.9], BSR = −6.20, $p < 0.001$) and controls (−5.6 [−9.6, −1.3], BSR = −2.65, $p=0.009$); and in NegAff for COVID-19 (+8.1 [+5.6, +10.5], BSR = 6.71 $p < 0.001$), although effects were non-significant for controls (+5.5 [−0.8, +12.3], BSR = 1.74, $p=0.074$). The average summary scores, however, were not significantly different between COVID-19 and control groups, as noted in Table 1.

TABLE 1 Summary of demographic and clinical data for study participants.

	Controls (N = 14)	COVID-19 (N = 54)	Group diff (SE)	Effect statistics	
				BSR	p-value
Years of Age, mean (SD)	40.8 (14.2)	40.9 (12.1)	0.1 (4.0)	0.03	0.986
Female, total (percent)	8/14 (57%)	36/53 (67%)	9.5 (14.5) %	0.65	0.495
Years of Education, mean (SD)	16.3 (2.4)	16.3 (2.2)	0.0 (0.7)	0.02	0.992
Days (symptom onset to scan)	194 [152, 235]	115 [75, 174]	-79 (29)	-2.67	0.011
Days (COVID test to scan)	151 [52, 235]	114 [71, 169]	-37 (42)	-0.89	0.361
Fever [ongoing]	0/14 (0%)	0/54 (0%)	- 11 (15)	- 0.77	- 0.414
[resolved]	8/14 (57%)	37/54 (69%)			
Cough [ongoing]	2/14 (14%)	8/54 (15%)	1 (10)	0.05	0.858
[resolved]	6/14 (43%)	30/54 (56%)	13 (15)	0.84	0.374
Sore throat [ongoing]	1/14 (7%)	2/54 (4%)	-3 (8)	-0.46	0.716
[resolved]	7/14 (50%)	38/54 (70%)	20 (15)	1.39	0.174
Shortness of breath [ongoing]	4/14 (29%)	13/54 (24%)	-5 (13)	-0.34	0.741
[resolved]	3/14 (21%)	18/54 (33%)	12 (13)	0.93	0.368
Excess fatigue [ongoing]	5/14 (36%)	17/54 (31%)	-4 (15)	-0.29	0.786
[resolved]	5/14 (36%)	32/54 (59%)	24 (15)	1.64	0.096
Gastrointestinal issues					
[ongoing]	3/14 (21%)	5/54 (9%)	-12 (12)	-1.07	0.299
[resolved]	3/14 (21%)	25/54 (46%)	25 (13)	1.88	0.074
Issues with smell/taste					
[ongoing]	1/14 (7%)	12/54 (22%)	15 (9)	1.68	0.122
[resolved]	4/14 (29%)	21/54 (39%)	10 (14)	0.75	0.453
Headache [ongoing]	0/14 (0%)	13/54 (24%)	24 (8)	4.21	<0.001
[resolved]	1/14 (7%)	10/54 (19%)	11 (9)	1.34	0.184
Symptom count (ongoing)	2.1 (2.4)	2.1 (2.3)	0.0 (0.7)	0.01	0.989
Symptom count (combined)	4.9 (3.8)	6.7 (2.8)	1.8 (1.0)	1.79	0.077
Social satisfaction summary	41.3 (13.1)	45.9 (8.9)	4.6 (3.7)	1.25	0.202
Well-being summary	44.4 (7.9)	44.2 (6.9)	-0.2 (2.3)	-0.08	0.928
Negative affect summary	55.5 (12.4)	58.1 (8.6)	2.6 (3.6)	0.72	0.464

The mean and standard deviation (SD) are reported for normally-distributed data, while the median is reported with lower and upper distribution quartiles [Q1, Q3] for non-normal data, and the proportion and percentage are reported for categorical data. For between-group comparisons, the mean difference and bootstrapped standard error (SE) are reported, along with the z-scored bootstrap ratio (BSR) and a percentile-based p-value.

3.2 Effects of COVID-19 on dMRI data

Voxel-wise analyses of the dMRI parameter maps are depicted in Figure 1. The COVID-19 group showed significant reductions in MD localized to the right anterior corona radiata (volume = 1701 mm³, center of mass = [21, 27, -9], peak BSR value = -4.24), splenium of the corpus callosum (1,350 mm³, [6, -39, 9], -5.62) and right posterior corona radiata (1,215 mm³, [30, -33, 21], -4.28) (Figure 1A); but no significant differences were observed for FA (95% interval of BSR values, computed over all voxels: [-1.59, 2.52]). Examining diffusion components, effects were significant for AD within the splenium of corpus callosum, including right superior (918 mm³, [15, -36, 30], -4.84) and medial aspects (918 mm³, [6, -39, 6], -7.09) and left sagittal stratum (1,161 mm³, [-48, -36, -12], -5.05) (Figure 1B), but non-significant for RD (95% interval of BSR values: [-2.74, 1.04]). Analyses of MK also found increased diffusion kurtosis in the medial aspect of splenium of corpus callosum (1863 mm³, [3, -36, 18], 4.54), left tapetum (1971 mm³, [-24, -42, 21], 4.03), and right posterior

corona radiata (1,053 mm³, [30, -36, 24], 4.12) (Figure 1C). For the NODDI parameters, no significant group differences were identified for ODI, V_{IC} or V_{ISO} (95% intervals of BSR values: [-1.86, 2.37], [-0.86, 2.41] and [-2.41, 1.28], respectively). Post-hoc analyses within the identified clusters found that results were not significantly influenced by supplementary clinical/demographic factors including ongoing symptom burden, initial symptom burden or time from symptom onset to MRI scan (see Appendix 3 for details).

3.3 Association of emotional health with dMRI data in COVID-19

Results of discriminant analysis on the NIH summary scores are depicted in Figure 2. Although individual scores were non-significant in Table 1, model testing revealed that the SocSat+NegAff model yielded the best explanatory power, with “next-best” model SocSat+WelBei+NegAff having moderately less support ($\Delta AICC = 2.06$, $L_{AICC,1} = 35.6\%$) and all

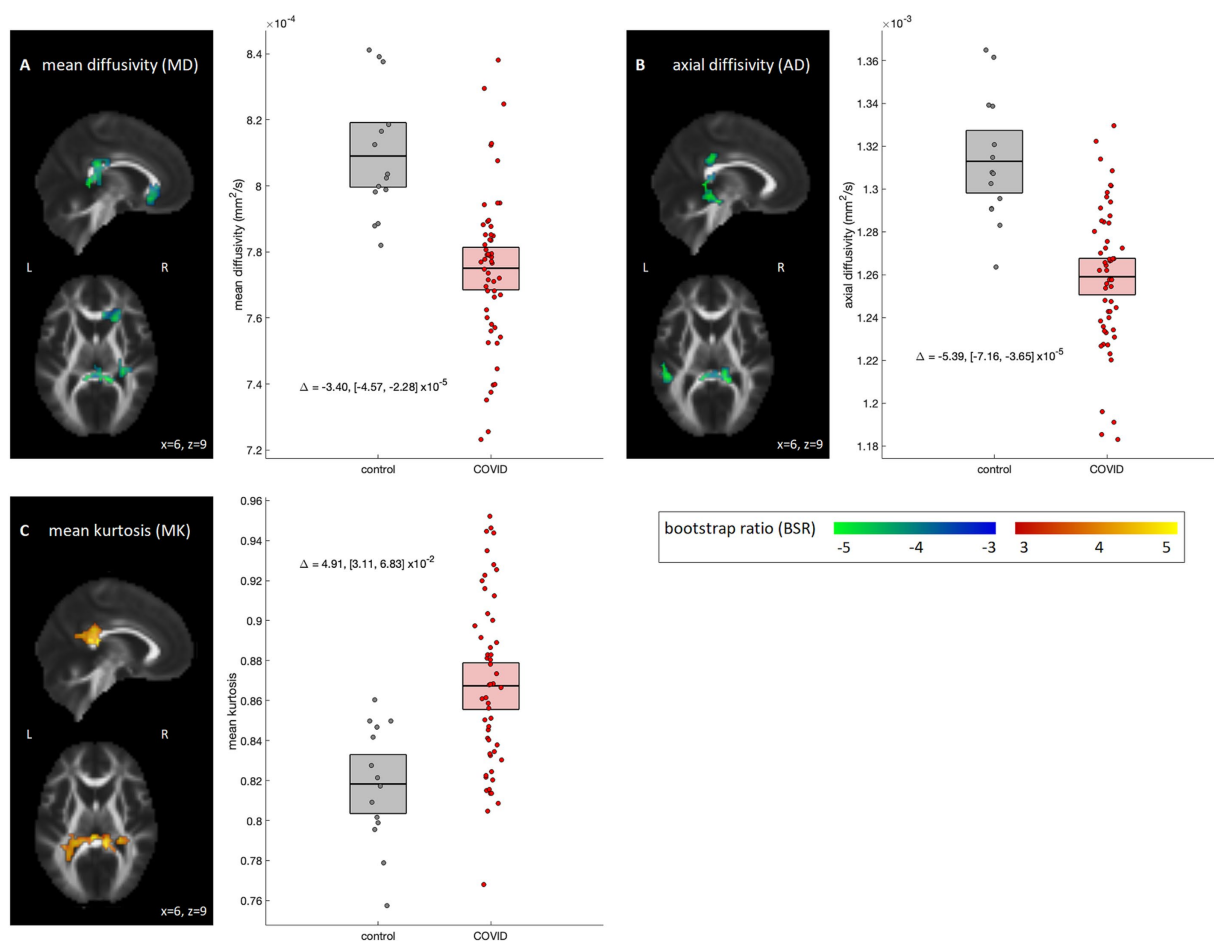


FIGURE 1

Diffusion MRI parameters showing significant differences between COVID-19 and control groups. Significant parameters include (A) mean diffusivity (MD), (B) axial diffusivity (AD) and (C) mean kurtosis (MK). For significant regions, standardized effect sizes in z-score scale via bootstrap ratio (BSR) values, displayed as maximum intensity projections in the sagittal and axial planes, overlaid on mean FA slices from Montreal Neurological Institute (MNI) coordinates ($x = 6, z = 9$). Group differences are shown as scatter plots, depicting the mean value within significant voxels for each participant. Boxes denote the mean and bootstrapped 95% confidence interval (95%CI) of the mean for each group. Group differences are also displayed as text, with bootstrapped 95% CIs.

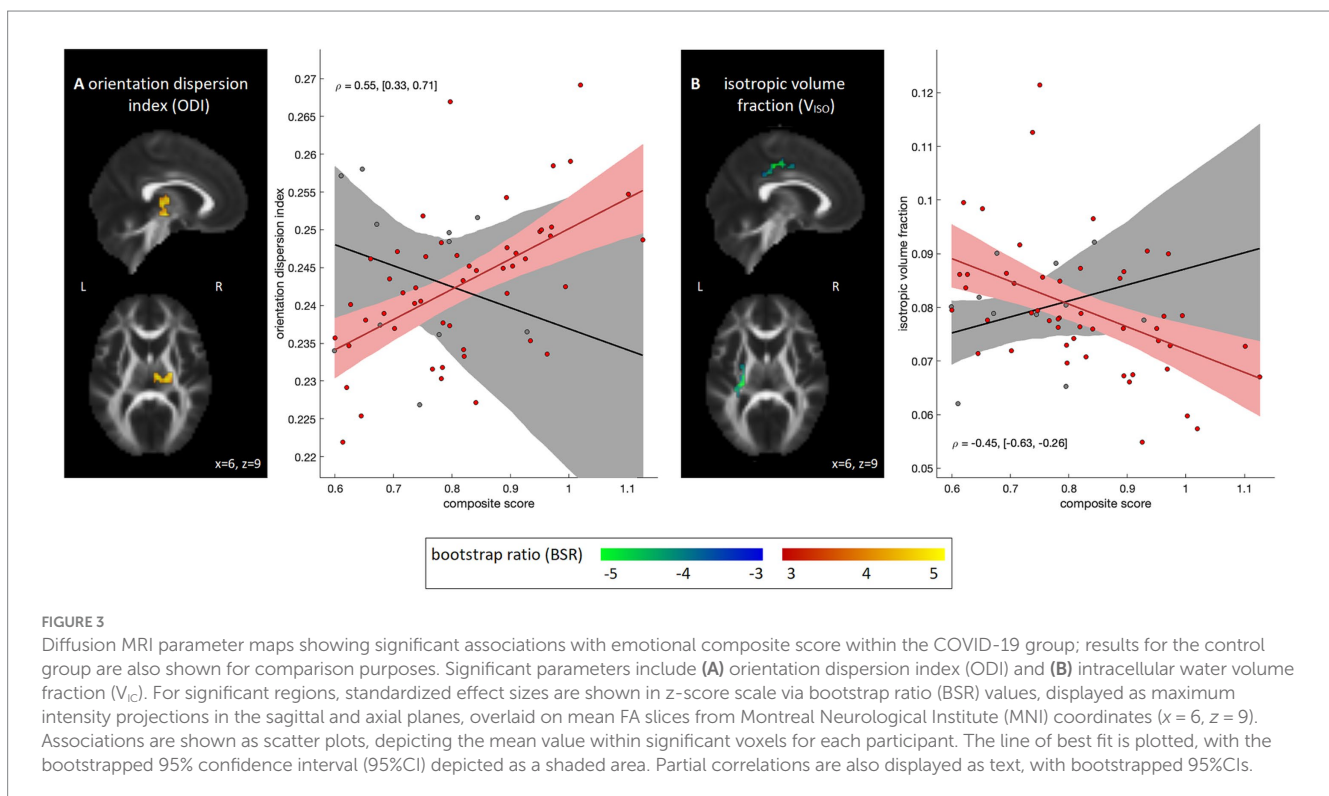
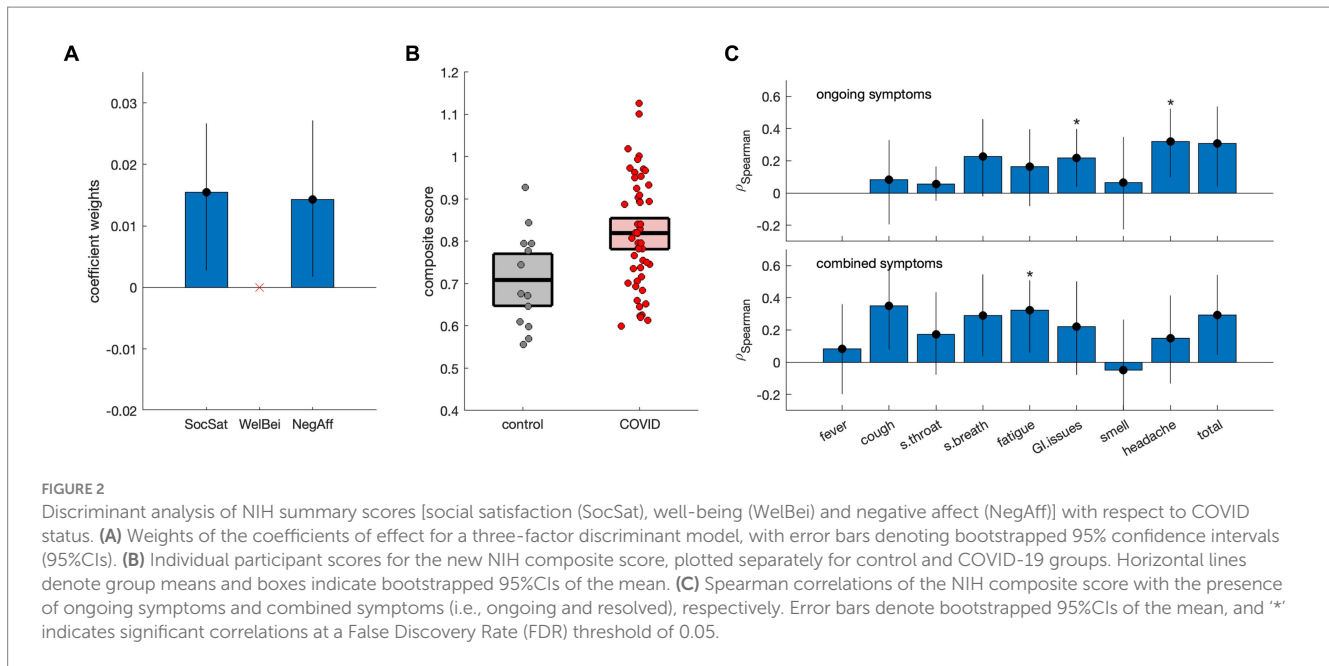
other models having substantially less support ($\Delta AIC_C \geq 3.36$, $L_{AIC_C} \leq 18.7\%$). Further testing affirmed that the SocSat+NegAff model best explained between-group differences (see Appendix 2 for details). As shown in Figure 2A, positive coefficient weights of comparable magnitude are obtained for SocSat (mean and 95%CI: 0.0158, [0.0027, 0.0267], BSR=2.63, $p=0.012$) and NegAff (0.0145, [0.0017, 0.0272], BSR=2.18, $p=0.024$). As shown in Figure 2B, this 2-variable model also produced elevated composite scores in the COVID-19 group (0.11, [0.04, 0.18], BSR=3.11, $p=0.002$), indicating higher relative values of both SocSat and NegAff for this group. In the COVID-19 group, positive correlations were also seen between the NIH emotional composite scores and the presence of viral symptoms (Figures 2C,D). At an FDR of 0.05, this included gastrointestinal issues (ongoing), headache (ongoing), and fatigue (combined). At an uncorrected $p < 0.05$, further effects were identified for cough (combined), shortness of breath (combined) and total symptoms (ongoing and combined).

Voxel-wise analyses correlating diffusion parameter data with the NIH composite scores are depicted in Figure 3. Within the COVID-19 group, no significant associations were identified for DTI measures of FA, MD, AD and RD after applying cluster-size thresholding (95%

intervals of BSR values: [-1.83, 2.25], [-2.45, 0.96], [-2.59, 1.16], and [-2.45, 1.17], respectively). Effects were similarly non-significant for MK. Among the NODDI measures, however, significant positive associations with ODI (Figure 3A) were seen within the right posterior limb of the internal capsule (1,296 mm³, [18, -21, 0], 4.50). In addition, significant negative associations with V_{ISO} were seen dorsally within the superior longitudinal fasciculus (volume = 1,052 mm³, center of mass = [-27, -24, 42], peak BSR value = 7.48), although effects for V_{IC} were non-significant (95% interval of BSR values: [-2.43, 1.66]). Post-hoc analyses within the identified clusters found that results were not significantly influenced by supplementary clinical/demographic factors including ongoing symptom burden, initial symptom burden or time from symptom onset to MRI scan (see Appendix 3 for details).

4 Discussion

This study found evidence of chronic differences in white matter microstructure among COVID-positive individuals with



persistent symptoms, relative to COVID-negative individuals with persistent viral symptoms. For DTI metrics, lower MD and AD values were identified, indicating reduced water diffusion, mainly along the primary diffusion axis. Conversely, neither FA nor RD yielded significant effects, indicating unreliable effects of COVID-19 status on the radial component of diffusion. The findings of reduced AD and MD suggest increased axonal pathology in the COVID-19 group relative to controls (36), e.g., axonal swelling and cytoskeletal disruption. Conversely, the absence of RD and FA effects suggests

a lack of support for altered myelination in the COVID-19 group (37).

These results are aligned with a study that compared individuals with PACS at 11 months post-infection (hospitalized and non-hospitalized) to uninfected controls (23). They also found reduced MD and AD, with affected regions including the corpus callosum and longitudinal fasciculus. Current results are also partially aligned with a study of hospitalized individuals with PACS at 3 months post-infection, which found reduced MD, AD and RD, and increased FA

(16). They also partly align with a study of non-hospitalized individuals with PACS at 6 months post-infection, which reported reduced MD and increased FA in multiple white matter tracts (19). However, other studies have observed reduced FA and increased diffusivity, in both hospitalized (18) and non-hospitalized (17) cohorts, suggesting heterogeneous post-COVID microstructural changes. In addition, a large prospective study of mainly non-hospitalized individuals, imaged an average of 4–5 months post-infection, reported areas of increased diffusivity relative to pre-infection imaging (14). Effects were spatially heterogeneous in the brain though, with diffusivity reductions also seen in many areas, including the splenium of the corpus callosum, posterior corona radiata and sagittal stratum. Previous studies have consistently found significant dMRI effects in COVID-19 survivors relative to uninfected controls; the present study extends these findings by identifying significant effects in COVID-positive individuals with persistent symptoms relative to COVID-negative individuals with similar symptoms.

The DTI results in this study are complemented by increased MK, indicating a greater departure from unrestricted Gaussian diffusion of water in these regions for the COVID-19 group. By contrast, NODDI analyses showed no significant alterations in ODI, V_{IC} or V_{ISO} . A previous study observed reduced V_{IC} , albeit for a mixed cohort of hospitalized and non-hospitalized individuals, compared to uninfected controls (15). Furthermore, microstructural effects of the previous study were smaller in individuals with shorter hospital stays (15), supporting the lack of findings in this study. In the previously noted large prospective study (14), altered ODI and V_{ISO} were seen relative to pre-infection imaging, although the magnitude and direction of effects showed high spatial variability in the brain. Collectively, dMRI findings of the present study suggest that the microstructural environment of white matter is altered for the COVID-19 group, but without substantial differences in tissue water contributions. As noted for the DTI parameters, this may represent axonal pathology, or alternatively, an accumulation of cellular debris following neuroinflammation. Based on post-hoc testing, group differences do not appear to be influenced by initial or ongoing viral symptom burden, nor time from symptom onset to imaging, replicating prior literature in PACS cohorts (23).

The present study also identified an NIH toolbox composite score of emotional health that distinguished the COVID-19 group from controls. Analyses of SocSat, WelBei and NegAff in isolation found that mean values tended to be lower than the normative mean for both groups, with no significant differences between COVID-19 and control groups. Multivariate analysis, however, showed significant positive effects of SocSat and NegAff when both were in the model. This may be interpreted as the COVID-positive individuals experiencing greater negative affect (i.e., sadness, fear, anger) after adjusting for level of social satisfaction. The interpretation is supported by positive associations between the composite score and self-reported COVID symptoms, with significant effects relating to headache and fatigue. Despite the latter associations, group differences in symptoms were not seen, except for ongoing headache. This is consistent with many symptoms being non-specific signs of viral infection (e.g., fever, cough, sore throat). Furthermore, non-headache symptoms more prevalent in COVID-19 (e.g., fatigue, hyposmia, hypogeusia) (7) may have effects mitigated by the relatively mild sequelae in the present cohort. This should be explored in future

research, with graded symptom scales providing more granular information that may better map onto NIH emotional scores.

Psychological effects are commonly reported in the acute phase of COVID-19 infection, including signs of depression, anxiety, and stress (38, 39). Among individuals with PACS, distress is similarly prevalent, often centered around a perceived lack of support and difficulty with daily activities (40) – such effects may be exacerbated by a persistent post-COVID inflammatory response (41). Interestingly, in the present cohort of non-hospitalized COVID-positive individuals, social satisfaction was not significantly lower than for controls. This highlights that COVID-negative individuals with viral symptoms may also have suffered from a perceived lack of support, given the widespread disruption of social systems during the pandemic (42–44), and that this should be acknowledged when characterizing mental health in COVID-19 research. The results provide evidence for a distinct pattern of emotional sequelae in COVID-positive individuals, compared to COVID-negative individuals with similar post-infection symptoms.

The study further identified significant correlations between dMRI parameters and the NIH emotional composite score in the COVID-19 group, supporting the presence of white matter abnormalities underlying the emotional sequelae. For DTI parameters and MK, no significant associations were identified. For the NODDI parameters, however, a significant positive association was seen with ODI, indicating greater dispersion of neurites within the identified regions. An increase in ODI has been linked to multiple chronic pathologies including demyelination (45), ischemic injury (46) and diffuse axonal injury (47), although the effects may also represent anatomical differences that predate COVID-19 infection. A negative association with V_{ISO} was also observed, indicating reduced extracellular free water within dorsal white matter. These results suggest accumulating intracellular water that is not neurite-specific, for individuals with prior COVID-19 infection and greater negative affect. Such results agree with animal models, in which neural injury is often accompanied by cellular swelling, glial hypertrophy and neuroplastic change, all of which may reduce extracellular free water (48). The present findings differ, however, from dMRI studies of chronic inflammation in other neurological conditions, which have reported increased free water (49, 50). A previous study of PACS also reported correlations with neuropsychiatric symptoms, albeit for standard DTI measures – they reported that FA of the sagittal stratum was correlated with fatigue, and MD of the amygdala was correlated with perceived stress (19). Despite the differing dMRI parameters and brain regions of interest, these results collectively support the interpretation that COVID-positive individuals endorsing higher emotional sequelae tend to have greater alterations in white matter microstructure.

Although significant effects of COVID-19 were identified for both clinical and neuroimaging indices, a discussion of study limitations is warranted. One such limitation is diagnostic uncertainty of the control group. While specificity of RT-PCR testing is high, studies have highlighted the often poor sensitivity of testing (51). Sensitivity is also time-dependent, with debate around the window of detectability (52). As such, there is a risk of false negatives in the control group, which may lead to under-estimating the effects of PACS on cerebral microstructure. This represents a challenge inherent to studies of COVID-19 with symptom-matched controls, and resolving the issue would require repeated RT-PCR testing conducted prospectively, or more restrictive selection criteria applied to COVID-negative controls. The sample sizes

are also limited, particularly for the control group, although given the lack of data assessing differences in dMRI and emotional health data for COVID-19 with persistent symptoms, relative to non-COVID infection, this represents a unique dataset. The more common literature practise is to contrast individuals who have recovered from COVID-19 against uninfected controls. The present study focused on differences in symptomatic individuals with and without COVID-19 diagnosis. However, it is unclear to what extent dMRI values in the control group are altered by infection, and whether dMRI alterations in the COVID-19 group are specific to PACS. To this end, future research should include additional control groups, e.g., consisting of non-infected individuals and COVID-infected individuals without persistent symptoms. Another important factor to consider is whether the presence of specific symptom complaints moderates the relationship between dMRI and emotional symptoms in PACS. For example, issues related to olfaction and headache may represent distinct forms of neural injury and/or have differing effects on emotional well-being. This will be an important consideration to investigate in future research. The observed white matter effects on emotional health may also be exacerbated by other processes such as metabolic dysfunction (53), altered brain function (54) and abnormal perfusion (55); future work in PACS should develop more complete models that incorporate these different processes, informed by multi-modal MRI. Lastly regarding dMRI parameters, it is important to emphasize that “standard” parameter settings were used for the NODDI model, which may not optimally capture post-COVID microstructural changes (56). Further work is needed to investigate their validity in this group and potentially refine the NODDI model for improved sensitivity to PACS effects.

In conclusion, the principal study finding was significantly altered water diffusion in the white matter of self-isolating COVID-positive individuals with persistent symptoms; this included reduced diffusivity, increased diffusion kurtosis and neurite dispersion. Distinct emotional sequelae were also identified among COVID-positive individuals, of increased negative affect after adjusting for social satisfaction. Negative affect in the COVID-19 group was further associated with neurite dispersion and reduced free water in white matter. These findings provide new insights into the emotional and pathophysiological correlates of persistent post-COVID symptoms.

Data availability statement

The datasets presented in this study can be found in online repositories. The names of the repository/repositories and accession number(s) can be found below: the datasets analyzed for this study can be found in the figshare data repository at: <https://doi.org/10.6084/m9.figshare.26036245>.

Ethics statement

The studies involving humans were approved by the Sunnybrook Health Sciences Centre ethics board. The studies were conducted in accordance with the local legislation and institutional requirements. The participants provided their written informed consent to participate in this study.

Author contributions

NC: Formal analysis, Methodology, Writing – original draft, Writing – review & editing. ER: Data curation, Methodology, Writing – review & editing. JC: Methodology, Writing – review & editing. AS: Methodology, Writing – review & editing. FG: Methodology, Writing – review & editing. MM: Methodology, Writing – review & editing. BL: Methodology, Writing – review & editing. IC: Methodology, Writing – review & editing. CH: Methodology, Writing – review & editing. SB: Methodology, Writing – review & editing. BM: Data curation, Methodology, Writing – review & editing. SG: Data curation, Methodology, Writing – review & editing. TS: Methodology, Writing – review & editing.

Funding

The author(s) declare that financial support was received for the research, authorship, and/or publication of this article. This study was funded in part by the Sunnybrook Foundation, the Dr. Sandra Black Centre for Brain Resilience & Recovery, a Canadian Institutes of Health Research (CIHR) Project Grant (165981), and a CIHR Operating Grant on Emerging COVID-19 Research Gaps and Priorities (177756).

Acknowledgments

The authors gratefully acknowledge Ms. Ruby Endre, Mr. Garry Detzler, and Mr. Sangkyu Moon for their work in imaging the research participants associated with the study. We also thank all participants who volunteered for the research.

Conflict of interest

The authors declare that the research was conducted in the absence of any commercial or financial relationships that could be construed as a potential conflict of interest.

Publisher's note

All claims expressed in this article are solely those of the authors and do not necessarily represent those of their affiliated organizations, or those of the publisher, the editors and the reviewers. Any product that may be evaluated in this article, or claim that may be made by its manufacturer, is not guaranteed or endorsed by the publisher.

Supplementary material

The Supplementary material for this article can be found online at: <https://www.frontiersin.org/articles/10.3389/fneur.2024.1432450/full#supplementary-material>

References

- Zhu N, Zhang D, Wang W, Li X, Yang B, Song J, et al. A novel coronavirus from patients with pneumonia in China, 2019. *N Engl J Med.* (2020) 382:727–33. doi: 10.1056/NEJMoa2001017
- Shah W, Heightman M, O'Brien S. UK guidelines for managing long-term effects of COVID-19. *Lancet.* (2021) 397:1706. doi: 10.1016/S0140-6736(21)00847-3
- World Health Organization. A clinical case definition of post COVID-19 condition by a Delphi consensus, 6 October 2021. (2021). Available at: https://www.who.int/publications/i/item/WHO-2019-nCoV-Post_COVID-19_condition-Clinical_case_definition-2021.1 (Accessed October 30, 2022).
- Nalbandian A, Sehgal K, Gupta A, Madhavan MV, Mcgroder C, Stevens JS, et al. Post-acute COVID-19 syndrome. *Nat Med.* (2021) 27:601–15. doi: 10.1038/s41591-021-01283-z
- Alkodaymi MS, Omrani OA, Fawzy NA, Abou Shaar B, Almamlouk R, Riaz M, et al. Prevalence of post-acute COVID-19 syndrome symptoms at different follow-up periods: a systematic review and meta-analysis. *Clin Microbiol Infect.* (2022) 28:657–66. doi: 10.1016/j.cmi.2022.01.014
- Baig AM, Khaleeq A, Ali U, Syeda H. Evidence of the COVID-19 virus targeting the CNS: tissue distribution, host–virus interaction, and proposed neurotropic mechanisms. *ACS Chem Neurosci.* (2020) 11:995–8. doi: 10.1021/acscchemneuro.0c00122
- Fernández-De-Las-Peñas C, Palacios-Ceña D, Gómez-Mayordomo V, Florencio LL, Cuadrado ML, Plaza-Manzano G, et al. Prevalence of post-COVID-19 symptoms in hospitalized and non-hospitalized COVID-19 survivors: a systematic review and meta-analysis. *Eur J Intern Med.* (2021) 92:55–70. doi: 10.1016/j.ejim.2021.06.009
- Sarbu N, Shih RY, Jones RV, Horkayne-Szakaly I, Oleaga L, Smirniotopoulos JG. White matter diseases with radiologic-pathologic correlation. *Radiographics.* (2016) 36:1426–47. doi: 10.1148/rg.2016160031
- Schmahmann JD, Smith EE, Eichler FS, Filley CM. Cerebral white matter: neuroanatomy, clinical neurology, and neurobehavioral correlates. *Ann N Y Acad Sci.* (2008) 1142:266–309. doi: 10.1196/annals.1444.017
- Dong Q, Welsh RC, Chenevert TL, Carlos RC, Maly-Sundgren P, Gomez-Hassan DM, et al. Clinical applications of diffusion tensor imaging. *J Magnet Reson Imaging.* (2004) 19:6–18. doi: 10.1002/jmri.10424
- Soares JM, Marques P, Alves V, Sousa N. A hitchhiker's guide to diffusion tensor imaging. *Front Neurosci.* (2013) 7:31. doi: 10.3389/fnins.2013.00031
- Steven AJ, Zhuo J, Melhem ER. Diffusion kurtosis imaging: an emerging technique for evaluating the microstructural environment of the brain. *Am J Roentgenol.* (2014) 202:W26–33. doi: 10.2214/AJR.13.11365
- Zhang H, Schneider T, Wheeler-Kingshott CA, Alexander DC. NODDI: practical in vivo neurite orientation dispersion and density imaging of the human brain. *NeuroImage.* (2012) 61:1000–16. doi: 10.1016/j.neuroimage.2012.03.072
- Douaud G, Lee S, Alfaro-Almagro F, Arthofer C, Wang C, McCarthy P, et al. SARS-CoV-2 is associated with changes in brain structure in UK biobank. *Nature.* (2022) 604:697–707. doi: 10.1038/s41586-022-04569-5
- Huang S, Zhou Z, Yang D, Zhao W, Zeng M, Xie X, et al. Persistent white matter changes in recovered COVID-19 patients at the 1-year follow-up. *Brain.* (2022) 145:1830–8. doi: 10.1093/brain/awab435
- Lu Y, Li X, Geng D, Mei N, Wu P-Y, Huang C-C, et al. Cerebral micro-structural changes in COVID-19 patients—an MRI-based 3-month follow-up study. *EClinicalMed.* (2020) 25:100484. doi: 10.1016/j.eclinm.2020.100484
- Pelizzari L, Cazzoli M, Lipari S, Laganà MM, Cabinio M, Isernia S, et al. Mid-term MRI evaluation reveals microstructural white matter alterations in COVID-19 fully recovered subjects with anosmia presentation. *Ther Adv Neurol Disord.* (2022) 15:175628642211119. doi: 10.1177/17562864221111995
- Qin Y, Wu J, Chen T, Li J, Zhang G, Wu D, et al. Long-term microstructure and cerebral blood flow changes in patients recovered from COVID-19 without neurological manifestations. *J Clin Invest.* (2021) 131:e147329. doi: 10.1172/JCI147329
- Liang H, Ernst T, Oishi K, Ryan MC, Herskovits E, Cunningham E, et al. Abnormal brain diffusivity in participants with persistent neuropsychiatric symptoms after COVID-19. *Neuroimmune Pharmacol Ther.* (2023) 37–48. doi: 10.1515/nipt-2022-0016
- Dantzer R, O'Connor JC, Freund GG, Johnson RW, Kelley KW. From inflammation to sickness and depression: when the immune system subjugates the brain. *Nat Rev Neurosci.* (2008) 9:46–56. doi: 10.1038/nrn2297
- Konsman JP, Parnet P, Dantzer R. Cytokine-induced sickness behaviour: mechanisms and implications. *Trends Neurosci.* (2002) 25:154–9. doi: 10.1016/S0166-2236(00)02088-9
- Gershon RC, Cella D, Fox NA, Havlik RJ, Hendrie HC, Wagster MV. Assessment of neurological and behavioural function: the NIH toolbox. *Lancet Neurol.* (2010) 9:138–9. doi: 10.1016/S1474-4422(09)70335-7
- Diez-Cirarda M, Yus M, Gómez-Ruiz N, Polidura C, Gil-Martínez L, Delgado-Alonso C, et al. Multimodal neuroimaging in post-COVID syndrome and correlation with cognition. *Brain.* (2023) 146:2142–52. doi: 10.1093/brain/awac384
- Macintosh BJ, Ji X, Chen JJ, Gilboa A, Roudaia E, Sekuler AB, et al. Brain structure and function in people recovering from COVID-19 after hospital discharge or self-isolation: a longitudinal observational study protocol. *Can Med Assoc Open Access J.* (2021) 9:e1114–9. doi: 10.9778/cmajo.20210023
- Public Health Ontario Coronavirus disease 2019 (COVID-19) – PCR. (2021). Available at: <https://www.publichealthontario.ca/en/laboratory-services/%20test-information-index/covid-19> (Accessed September 30, 2022).
- Ontario COVID-19 Science Advisory Table. (2022). Ontario dashboard: percentage of cases caused by different variants in Ontario. Public Health Ontario (PHO).
- Office of the Premier. Ontario moving to phase two of COVID-19 vaccine distribution plan. Ontario (2021).
- Zhang S, Arfanakis K. Investigating the role of ICBM-space human brain diffusion tensor templates in inter-subject spatial normalization. *Proc Intl Soc Mag Reson Med.* (2011) 344
- Salsman JM, Butt Z, Pilkonis PA, Cyranowski JM, Zill N, Hendrie HC, et al. Emotion assessment using the NIH toolbox. *Neurology.* (2013) 80:576–86. doi: 10.1212/WNL.0b013e3182872e11
- Efron B, Tibshirani RJ. An introduction to the bootstrap. New York: Chapman and Hall/CRC (1994).
- Sadooghi-Alvandi S, Jafari AA. A parametric bootstrap approach for one-way ANCOVA with unequal variances. *Commun Stat Theory Methods.* (2013) 42:2473–98. doi: 10.1080/03610926.2011.625486
- Kodiweera C, Alexander AL, Harezlak J, McAllister TW, Wu Y-C. Age effects and sex differences in human brain white matter of young to middle-aged adults: a DTI, NODDI, and q-space study. *NeuroImage.* (2016) 128:180–92. doi: 10.1016/j.neuroimage.2015.12.033
- Salat DH, Lee SY, Yu P, Setty B, Rosas HD, Grant PE. DTI in development and aging. *Diffusion MRI.* (2009) 1:205–36. doi: 10.1016/B978-0-12-374709-9.00010-9
- Szeszko PR, Vogel J, Ashtari M, Malhotra AK, Bates J, Kane JM, et al. Sex differences in frontal lobe white matter microstructure: a DTI study. *Neuroreport.* (2003) 14:2469–73. doi: 10.1097/00001756-200312190-00035
- Anderson D, Burnham K. Model selection and multi-model inference, vol. 63. Second ed. NY: Springer-Verlag (2004). 10 p.
- Song S-K, Sun S-W, Ju W-K, Lin S-J, Cross AH, Neufeld AH. Diffusion tensor imaging detects and differentiates axon and myelin degeneration in mouse optic nerve after retinal ischemia. *NeuroImage.* (2003) 20:1714–22. doi: 10.1016/j.neuroimage.2003.07.005
- Song S-K, Yoshino J, Le TQ, Lin S-J, Sun S-W, Cross AH, et al. Demyelination increases radial diffusivity in corpus callosum of mouse brain. *NeuroImage.* (2005) 26:132–40. doi: 10.1016/j.neuroimage.2005.01.028
- Bo H-X, Li W, Yang Y, Wang Y, Zhang Q, Cheung T, et al. Posttraumatic stress symptoms and attitude toward crisis mental health services among clinically stable patients with COVID-19 in China. *Psychol Med.* (2021) 51:1052–3. doi: 10.1017/S0033291720000999
- Hao F, Tam W, Hu X, Tan W, Jiang L, Jiang X, et al. A quantitative and qualitative study on the neuropsychiatric sequelae of acutely ill COVID-19 inpatients in isolation facilities. *Transl Psychiatry.* (2020) 10:1–14. doi: 10.1038/s41398-020-01039-2
- Leviner S. Recognizing the clinical sequelae of COVID-19 in adults: COVID-19 long-haulers. *J Nurse Pract.* (2021) 17:946–9. doi: 10.1016/j.nurpra.2021.05.003
- Mazza MG, De Lorenzo R, Conte C, Poletti S, Vai B, Bollettini I, et al. Anxiety and depression in COVID-19 survivors: role of inflammatory and clinical predictors. *Brain Behav Immun.* (2020) 89:594–600. doi: 10.1016/j.bbi.2020.07.037
- Ao Y, Zhu H, Meng F, Wang Y, Ye G, Yang L, et al. The impact of social support on public anxiety amidst the COVID-19 pandemic in China. *Int J Environ Res Public Health.* (2020) 17:9097. doi: 10.3390/ijerph17239097
- Szkody E, Stearns M, Stanhope L, McKinney C. Stress-buffering role of social support during COVID-19. *Fam Process.* (2021) 60:1002–15. doi: 10.1111/famp.12618
- Xiao H, Zhang Y, Kong D, Li S, Yang N. The effects of social support on sleep quality of medical staff treating patients with coronavirus disease 2019 (COVID-19) in January and February 2020 in China. *Med Sci Monitor.* (2020) 26:e923549-41. doi: 10.12659/MSM.923549
- Grussu F, Schneider T, Tur C, Yates RL, Tachrount M, İanuș A, et al. Neurite dispersion: a new marker of multiple sclerosis spinal cord pathology? *Ann Clin Trans Neurol.* (2017) 4:663–79. doi: 10.1002/acn3.445
- Mastropietro A, Rizzo G, Fontana L, Figini M, Bernardini B, Straffi L, et al. Microstructural characterization of corticospinal tract in subacute and chronic stroke patients with distal lesions by means of advanced diffusion MRI. *Neuroradiology.* (2019) 61:1033–45. doi: 10.1007/s00234-019-02249-2
- Churchill NW, Caverzasi E, Graham SJ, Hutchison MG, Schweizer TA. White matter during concussion recovery: comparing diffusion tensor imaging (DTI) and

- neurite orientation dispersion and density imaging (NODDI). *Hum Brain Mapp.* (2019) 40:1908–18. doi: 10.1002/hbm.24500
48. Syková E, Nicholson C. Diffusion in brain extracellular space. *Physiol Rev.* (2008) 88:1277–340. doi: 10.1152/physrev.00027.2007
49. Di Biase MA, Zalesky A, Cetin-Karayumak S, Rath Y, Lv J, Boerrigter D, et al. Large-scale evidence for an association between peripheral inflammation and white matter free water in schizophrenia and healthy individuals. *Schizophr Bull.* (2021) 47:542–51. doi: 10.1093/schbul/sbaa134
50. Pasternak O, Kubicki M, Shenton ME. In vivo imaging of neuroinflammation in schizophrenia. *Schizophr Res.* (2016) 173:200–12. doi: 10.1016/j.schres.2015.05.034
51. Pecoraro V, Negro A, Pirotti T, Trenti T. Estimate false-negative RT-PCR rates for SARS-CoV-2. A systematic review and meta-analysis. *Eur J Clin Investig.* (2022) 52:e13706. doi: 10.1111/eci.13706
52. Mina MJ, Parker R, Larremore DB. Rethinking Covid-19 test sensitivity—a strategy for containment. *N Engl J Med.* (2020) 383:e120. doi: 10.1056/NEJMp2025631
53. Ernst T, Ryan MC, Liang H-J, Wang JP, Cunningham E, Saleh MG, et al. Neuronal and glial metabolite abnormalities in participants with persistent neuropsychiatric symptoms after COVID-19: a brain proton magnetic resonance spectroscopy study. *J Infect Dis.* (2023) 228:1559–70. doi: 10.1093/infdis/jiad309
54. Chang L, Ryan MC, Liang H, Zhang X, Cunningham E, Wang J, et al. Changes in brain activation patterns during working memory tasks in people with post-COVID condition and persistent neuropsychiatric symptoms. *Neurology.* (2023) 100:e2409–23. doi: 10.1212/WNL.0000000000207309
55. Kim WS, Ji X, Roudaia E, Chen JJ, Gilboa A, Sekuler A, et al. MRI assessment of cerebral blood flow in nonhospitalized adults who self-isolated due to COVID-19. *J Magn Reson Imaging.* (2023) 58:593–602. doi: 10.1002/jmri.28555
56. Hutchinson EB, Avram AV, Irfanoglu MO, Koay CG, Barnett AS, Komlos ME, et al. Analysis of the effects of noise, DWI sampling, and value of assumed parameters in diffusion MRI models. *Magn Reson Med.* (2017) 78:1767–80. doi: 10.1002/mrm.26575